Electronic Supplementary Information

Tuned interfacial charge tansport via Ti-O-Sn bonds for efficient CO_2 conversion

Shikang Yin,[a,c] Fan Zhou,[a] Yiying Zhou,[a] Yuming Sun,[a] Binrong Li,*[b] Yingying Qin,*[c] Yan Yan,*[a] Pengwei Huo,*[a]

[a]*Institute of Green Chemistry and Chemical Technology, School of Chemistry and Chemical Engineering, Jiangsu University, Zhenjiang 212013, PR China,*

[b]*National and Local Joint Engineering Laboratory of Municipal Sewage Resource Utilization Technology, School of Environmental Science and Engineering, Suzhou University of Science and Technology, Suzhou 215009, P.R. China,*

[c]*Department of Applied Biology and Chemical Technology and Research Institute for Smart Energy, the Hong Kong Polytechnic University, Hung Hom, Hong Kong, PR China.*

*** Corresponding authors:**

B. Li (libr@usts.edu.cn)
Y. Qin (yingying.qin@polyu.edu.cn)
Y. Yan (dgy5212004@163.com)
P. Huo (huopw@ujs.edu.cn)

1.Experimental

1.1. Materials

Tin chloride pentahydrate ($SnCl_4 \cdot 5H_2O$), aluminum carbide titanium (Ti_3AlC_2), hydrofluoric acid (HF, 40%), L-cysteine ($C_3H_7NO_2S$), sodium dodecyl benzenesulfonate (SDBS), ethylene glycol ($C_2H_6O_2$) and ethanol (C_2H_5OH) were all purchased from Sinopharm Chemical Reagent Co., Ltd. (Shanghai, China). The de-ionized (DI) water used throughout the experiment came from purified local water. All analytical grade chemical reagents were used directly without further purification.

1.2. Preparation of the samples

1.2.1. Preparation of MXene

The typical synthesis process of MXene (Ti_3C_2) was as follows: 2 g Ti_3AlC_2 powder was added to 10 mL of hydrofluoric acid solution and kept stirring for 48 h. Subsequently, the acidic solid residue was washed several times with deionized water by centrifugation until the pH of the solution reached around 7. The obtained Ti_3C_2 was dispersed in 100 mL of deionized water and sonicated for 1 h (3500 rpm/min) under N_2 atmosphere to collect a single layer of Ti_3C_2 material.

1.2.2. Preparation of atomic layer SnS_2

A typical modified solvothermal process, 0.0877g $SnCl_4 \cdot 5H_2O$, 0.2091g SDBS and 0.2423g $C_3H_7NO_2$ were dissolved in a mixed solution of DI water (15 mL) and ethylene glycol (15 mL), and stirred for 20 min. Then, the homogeneous mixed solution was transferred to a 50 mL autocalve, sealed and heated at 160 °C for 10 h. Then, the system was naturally cooled to room temperature, the precipitate was collected by centrifugation, washed with ethanol and DI water for several times, and then put it into a vacuum drying oven at 60 °C for12 h.

1.2.3. Preparation of SnS_2/MXene composite

SnS_2/MXene was synthesized as follows: 0.0877g $SnCl_4 \cdot 5H_2O$ was dissolved in a mixed solution of ethylene glycol (15 mL) and DI water (15 mL) of 50 ml the beaker, and then a certain amount (1%, 3%, 5%, 7%) of MXene aqueous solution (1 mg/mL) was ultrasonicated for 0.5 h, and then added to the above solution. Next, stirred for 15 min to form a uniform solution. 0.2091g SDBS and 0.2423g $C_3H_7NO_2$ were added in the above mixed solution, and stirred for 20 min to form a uniform solution. Next, the mixed solution was transferred to a 50 mL autocalve, sealed and heated at 160 °C for 10 h. Then, the system was naturally cooled to room temperature, the precipitate was collected by centrifugation, washed with ethanol and DI water for several times, and then put it into a vacuum drying oven at 60 °C for12 h.

1. Characterization:

The crystal structure and elemental orbital information of the catalyst were examined by X-ray diffraction (XRD, model MAC Science, Japan) and X-ray photoelectron spectroscopy (XPS, PHI 5300, PerkinElmer), respectively. The vibrational modes of the catalyst were investigated by Raman spectroscopy (Thermo Fisher, America). The microscopic of the catalyst was investigated by scanning electron microscopy (SEM, JEM-7800F, Japan), high-resolution transmission electron microscopy (HR-TEM, JEM-2010, Japan). The thickness of the samples was observed using Atomic Force Microscopy (AFM, MFP-3D, America). The ultraviolet-visible diffuse reflectance spectroscopy (DRS, Shimadzu UV-3600) was used to study the absorption bands of the catalysts. The photoluminescence spectra of the catalysts were studied on a luminescence spectrometer (F-4500 Hitachi, Japan). The specific surface area and pore size distribution of the material were characterized by Brunauer-Emmett-Teller (BET) technique and Barrett-Joiner-Halenda (BJH) method, respectively. The reaction process of photoreduction of CO_2 was investigated using in-situ diffuse reflectance Fourier transform infrared spectroscopy (Nicolet iS10). The isotope-labeled experiments were performed using $^{13}CO_2$ instead of $^{12}CO_2$, and the products were analyzed using gas chromatography-mass spectrometry (GC-MS, 7890A and 5975C, Agilent).

2. Photo-electrochemical test:

Obtained photoelectric characterization data based on electrochemical system (CHI 660B, Shanghai, China). The measurement system includes 0.5 M Na_2SO_4 electrolyte solution, 300W Xenon lamp, Pt electrode, calomel electrode (SCE), potassium ferricyanide solution, conductive glass, light barrier.

3. Photocatalytic tests

The activity of the catalyst was evaluated by the photoreduction CO_2 reaction. 5 mg of the catalyst was dispersed on quartz glass, and it was put into the bottom of a 150 ml reactor, and 2 ml of deionized water was added. Before light exposure, CO_2 (99.999%) gas was introduced into the reactor and bubbled for 20 min to exhaust the air, and maintain the normal pressure of the system. The products were taken from the reactor every 1 h, and the type and content of the product were analyzed by a gas chromatograph (GC-7920, China) equipped with thermal conductivity detector (TCD) and hydrogen flame ionization detector (FID).

4. Computational Details

All the density functional theory (DFT) calculations were performed for structural optimization as implemented in the Vienna ab-initio Simulation Package (VASP). The PBE exchange-correlation functional of the generalized gradient approximation (GGA) was used to describe the exchange correlation energy. A plane-wave kinetic-energy cutoff of 400 eV and a maximum force tolerance of 0.05 eV/Å were employed to

obtain well-converged results. A vacuum thickness of 20 Å was used in z-direction to avoid interactions between periodic slab images.

The free energy change (ΔG) for adsorptions were determined as follows:

$$\Delta G = E_{total} - E_{slab} - E_{sub} + \Delta EZPE - T\Delta S$$

where Etotal is the total energy for the adsorption state, Eslab is the energy of pure surface, Esub is the energy of the adsorption substrate, ΔEZPE is the zero-point energy change and ΔS is the entropy change.

Supplementary Figures

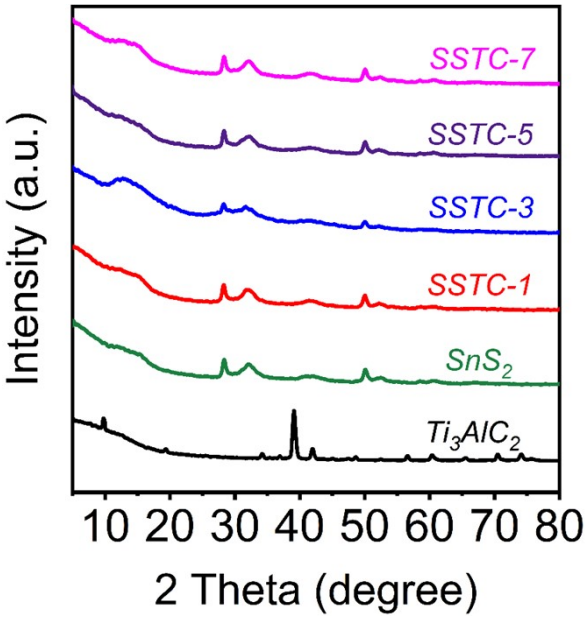

Fig. S1 XRD pattern of the Ti_3C_2, SnS_2 and SSTC-X (X=1, 3, 5, 7) samples.

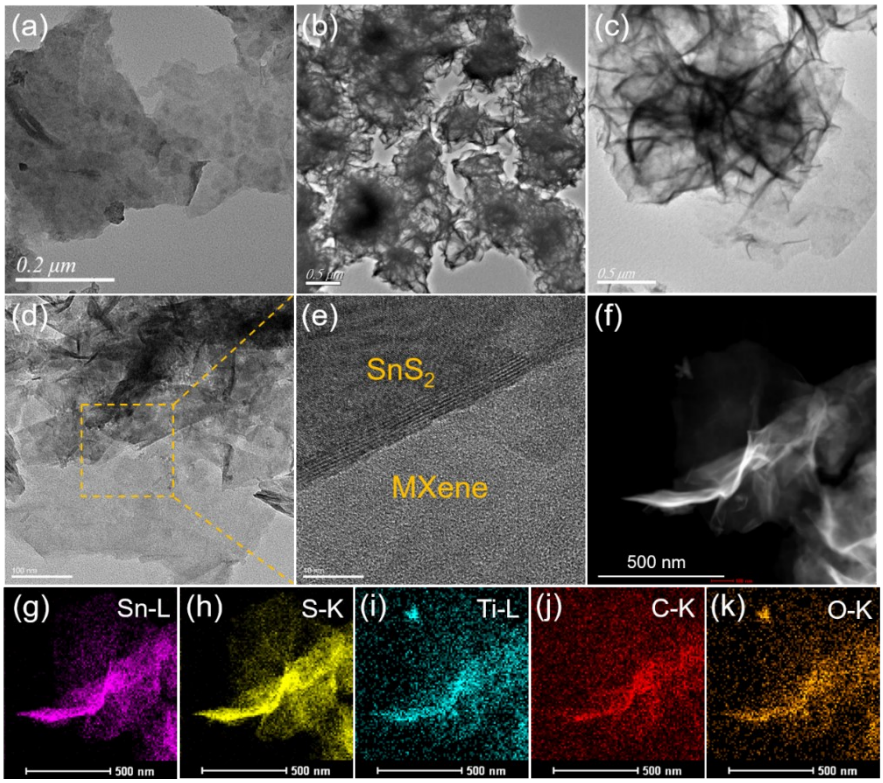

Fig. S2 (a) TEM image of Ti_3C_2 sample; **(b)** TEM image of the SnS_2 catalyst; (**c, d**) TEM image of the SSTC-5 catalyst; **(e)** HRTEM image of the SSTC-5 catalyst; **(f)** HAADF-STEM image: corresponding Sn **(g)**, S **(h)**, Ti **(i)**, C **(j)**, O **(k)** element mapping of SSTC-5 catalyst, respectively.

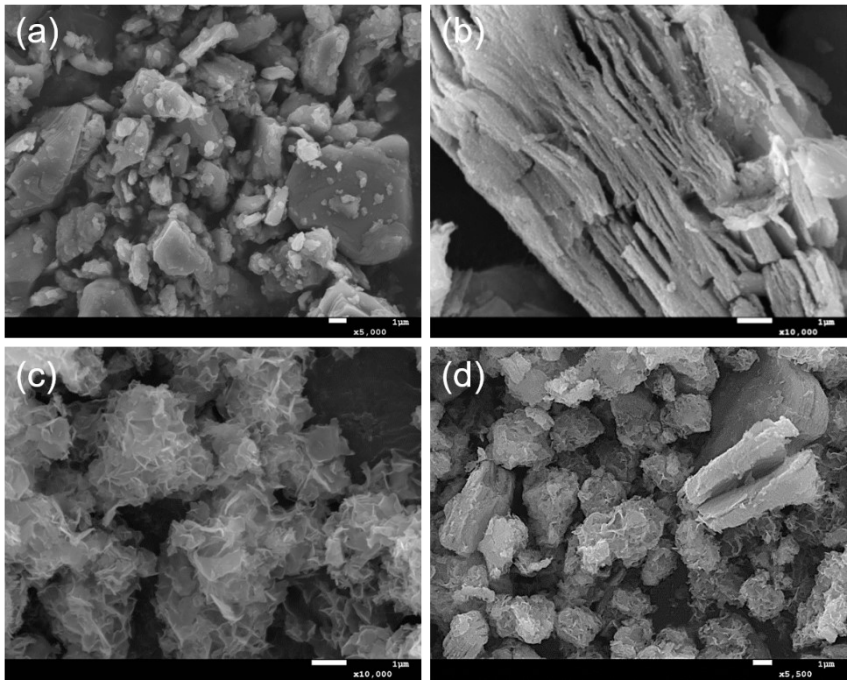

Fig. S3 SEM image of the Ti_3AlC_2 (a), Ti_3C_2 (b), SnS_2 (c) and SSTC-5 (d) catalyst, respectively.

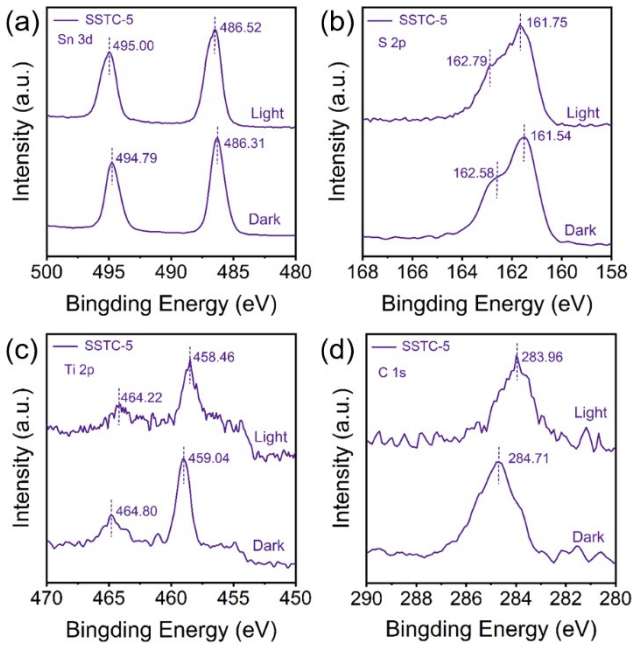

Fig. S4 In-situ XPS spectroscopy characterization of SSTC-5 catalyst: The Sn_{3d} orbits **(a)**, S_{2p} orbits **(b)**, Ti_{2p} orbits **(c)** and C_{1s} orbits **(d)** of the SSTC-5 samples were compared under the dark and light conditions.

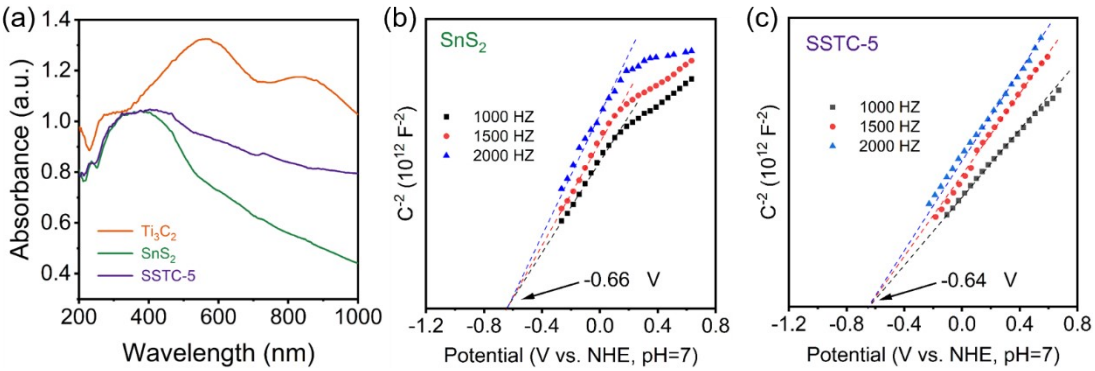

Fig. S5 (a) UV-Vis DRS spectra of the Ti_3C_2, SnS_2 and SSTC-5 catalyst; Mott-Schottky curve of SnS_2 (b) and SSTC-5 (c) catalyst.

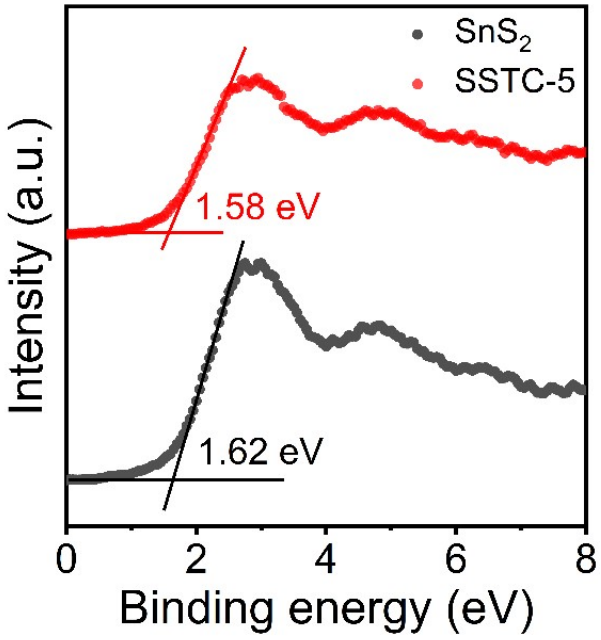

Fig. S6 XPS valence band spectra of SnS_2 and SSTC-5 composites.

The optical properties of Ti_3C_2, SnS_2 and SSTC-5 composites were studied by UV-Vis DRS spectroscopy (Fig. S5a). Ti_3C_2 has a strong photoresponse at 590 nm and 850 nm, with the absorption at 590 nm corresponding to the intrinsic properties of Ti_3C_2, while the light response at 850 nm corresponds to the plasmon resonance effect (LSPR) of Ti_3C_2. SnS_2 showed strong light response in the absorption range of 350-600 nm, and when Ti_3C_2 was added, the light absorption range of SSTC-5 composites was significantly broadened, and the response ability of the whole visible light range was improved. Furthermore, the conduction band potentials of the SnS_2 and SSTC-5 composites was investigated by a Mott-Schottky curve (Figs. S5b, S5c). The results showed that the conduction band potentials of SnS_2 and SSTC-5 were -0.66 V and -0.64 V, respectively, indicating that Ti_3C_2 did not significantly change the conduction band position of the SnS_2 material. At the same time, the valence band positions of SnS_2 and SSTC-5 were 1.62 eV and 1.58 eV, respectively (Fig. S6). Clearly, the redox capacity of the prepared samples can drive water oxidation and CO_2 reduction.

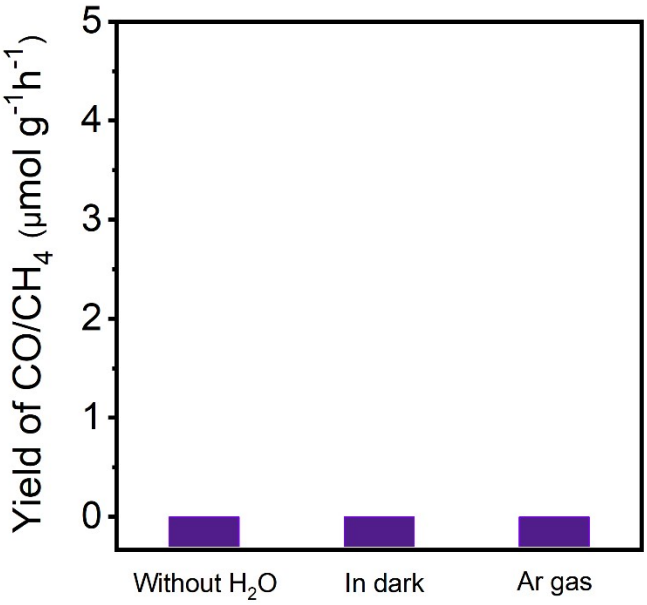

Fig. S7 Control experiments with SSTC-5 catalyst in the absence of H_2O, in the dark, or in Ar gas.

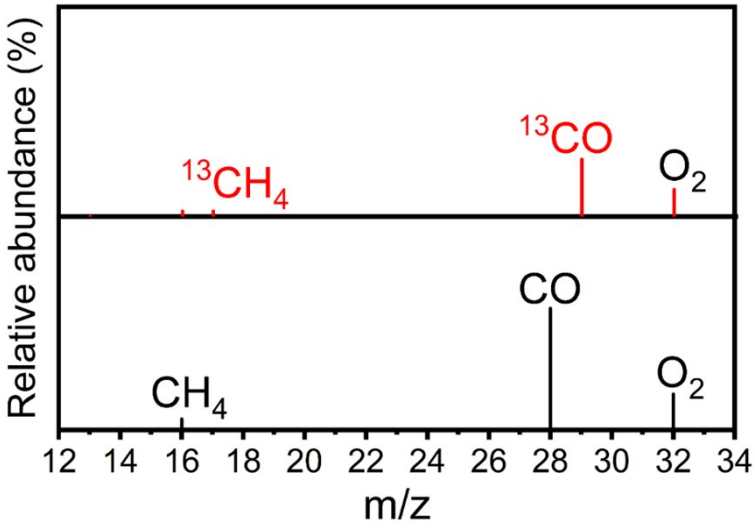

Fig. S8 Mass spectrum (m/z =28, 29) analyses of ^{12}CO and ^{13}CO in the overall CO_2 photoreduction on the SSTC-5 catalyst.

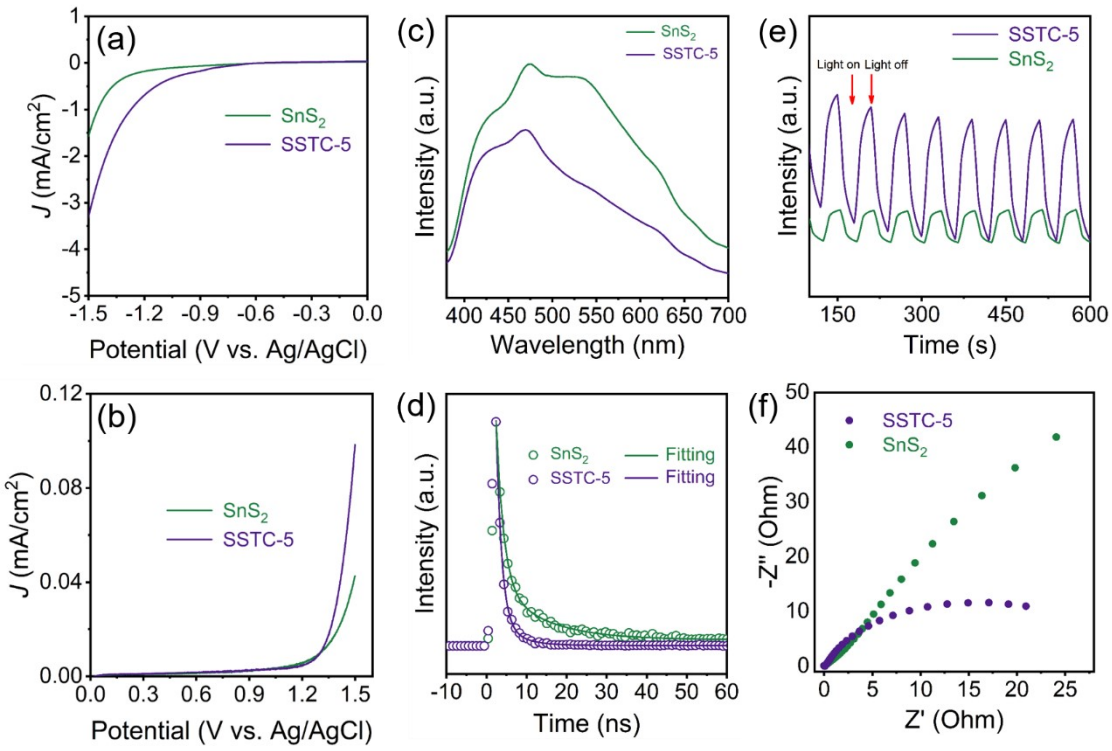

Fig. S9 (a, b) Linear sweep voltammogram of the SnS_2 and SSTC-5 catalysts; **(c, d)** Steady-state fluorescence (PL) and transient fluorescence (FL) of SnS_2 and SSTC-5 catalysts of SnS_2 and SSTC-5 catalysts (excitation wavelength: 362 nm); **(e, f)** The transient photocurrent response and electrochemical impedance spectroscopy of SnS_2 and SSTC-5 catalysts.

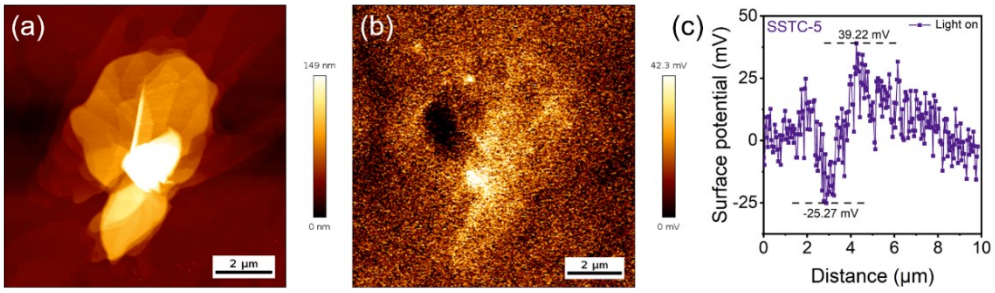

Fig. S10 Kelvin probe force microscope images of SSTC-5 catalyst in the dark **(a)** and in the light **(b)**; Surface potential analysis of SSTC-5 catalyst **(c)**.

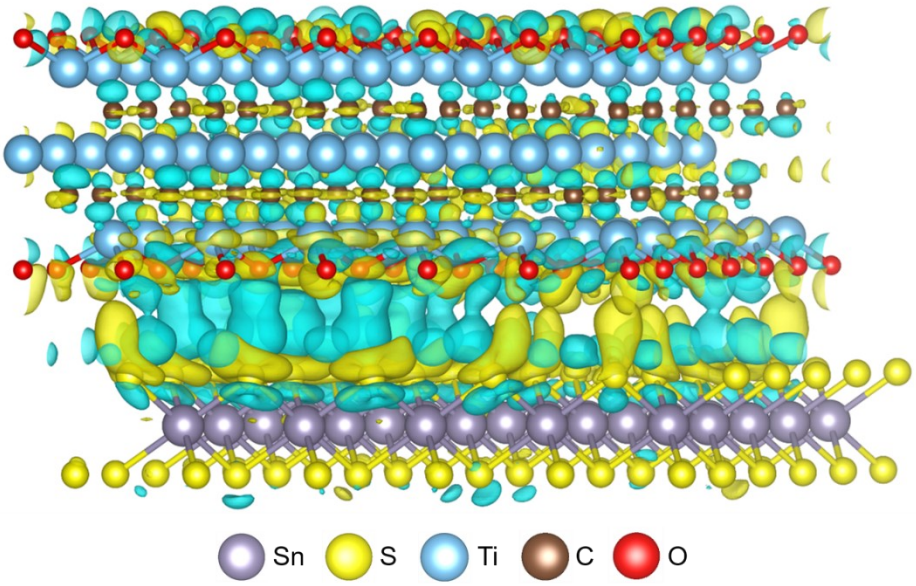

Fig. S11 Differential charge of SnS_2/Ti_3C_2 composite catalysts. (Yellow represents charge accumulation and blue represents charge consumption)

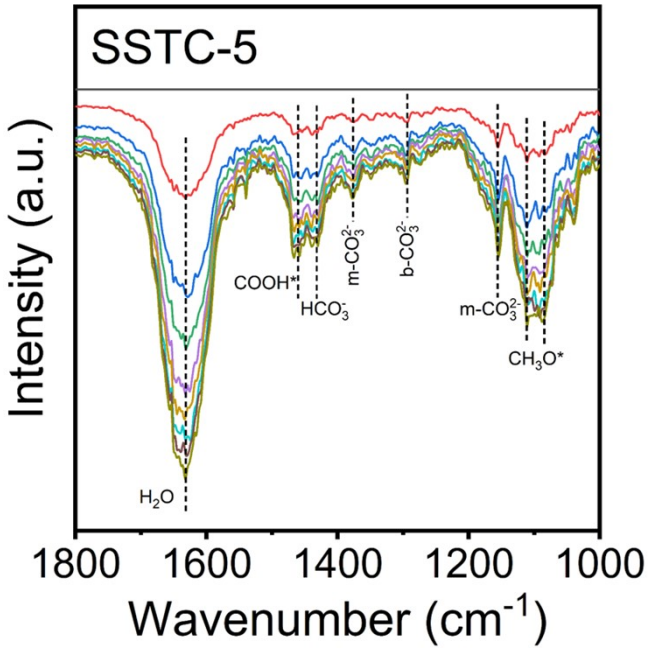

Fig. S12 DRIFTS spectra collected from the CO_2/H_2O/SSTC-5 interface under constant 450 nm irradiation in 15 min (3W, LED).

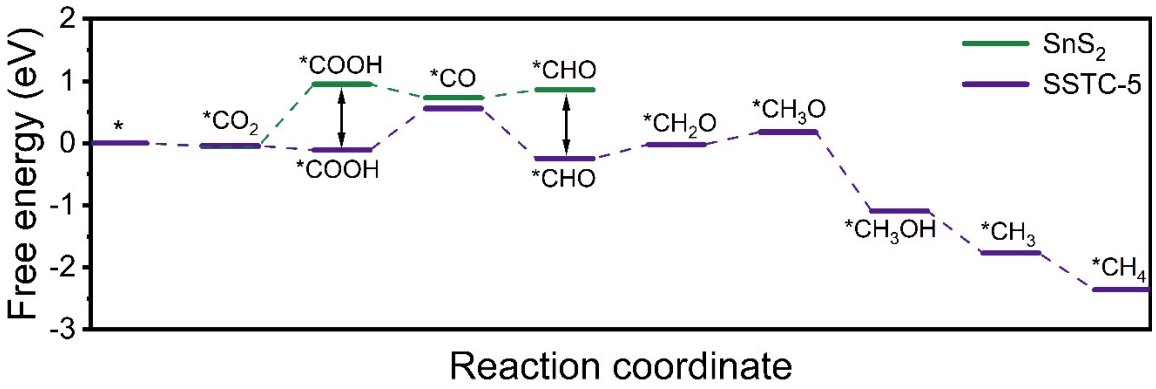

Fig. S13 Gibbs free energy of photoreduction of CO_2 over SnS_2 and SSTC-5 catalysts.